CHEMICAL ENGINEERING TRANSACTIONS
VOL. 96, 2022
A publication of AIDIC
The Italian Association of Chemical Engineering
Online at www.cetjournal.it
Guest Editors: David Bogle, Flavio Manenti, Piero Salatino

ISBN 978-88-95608-95-2; **ISSN** 2283-9216
DOI: 10.3303/CET2296079

Hydrothermal Conversion of Black Liquor to Magnetic Hydrochar and its Potential for Methylene Blue Removal

Bich N. Nguyen[a,b]*, Nghi H. Nguyen[b], Phuong T.Q. Phan[c], Tung C.T. Pham[a,d], Thanh D. Nguyen[a,c], Nguyen S. Pham[e], Anh Q.K. Nguyen[e]*

[a]Graduate University of Science and Technology, Viet Nam Academy of Science and Technology, Hanoi City, 100000, Vietnam
[b]Dong Thap University, Cao Lanh City, 870000, Vietnam
[c]Institute of Applied Materials Science, Viet Nam Academy of Science and Technology, Ho Chi Minh City, 700000, Vietnam
[d]Institute of Chemical Technology, Viet Nam Academy of Science and Technology, Ho Chi Minh City, 700000, Vietnam
[e]Institute of Applied Technology and Sustainable Development, Nguyen Tat Thanh University, Ho Chi Minh City, Vietnam
nnbich@dthu.edu.vn, nqkanh@ntt.edu.vn

With rapid industrial development, many contaminants have been released into the environment, putting human health in risk. Black liquor is plentiful in organic and inorganic contaminants that deplete oxygen levels in water bodies and harm aquatic life. Herein, black liquor was utilized as a precursor to fabricate magnetic hydrochar using a one-step hydrothermal method. Multiple technologies were carried out to characterize the physicochemical properties of the as-prepared samples. As a result, the best magnetic hydrochar (using 1 M Fe^{3+}) with spherical microparticles (approximately 50 - 120 nm), specific surface area (171.4 m^2 g^{-1}), total pore volume (0.146 cm^3 g^{-1}) and saturated magnetization (33.7 emu g^{-1}) was discovered. Furthermore, its adsorption capacity was 97.40 mg g^{-1} and the reusability remained around 83.19 % after 5 times. The research could lead a novel, cost-effective, and environmentally friendly method of utilizing agricultural waste for aquatic environment remediation.

1. Introduction

The scarcity of water potential and rapid industrialization are currently the two leading causes of eroding water quality (Titchou et al., 2021, Pham et al., 2022). Hence, prior to discharging waste effluents into nature, appropriate treatment must be applied (Zhang et al., 2021, Pham and Le, 2022). Adsorption is a ground-breaking process for removing contaminants from polluted effluents before they enter the aquatic environment (Le et al., 2021). Among a wide range of water contaminants, methylene blue (MB) is poisonous and non-biodegradable, posing a serious threat to human health and pollution prevention (Yağmur and Kaya, 2021). Additionally, paper-manufacturing industries use rice straw (RS) as raw material, resulting in a large amount of black liquor, which must be treated before it comes into contact with water (Tawfik et al., 2021). Black liquor is primarily high in organic pollutants, which can be exploited to produce useful byproducts and meet sustainability goals (Valderrama et al., 2021). Hydrochar, a type of stable organic substance produced from biomass at moderately low temperature (453 - 623 K), has wide range of application (Sharma et al., 2020). Typically, hydrochar was produced from the pyrolysis (at temperatures up to 1173 K). Hydrothermal carbonization, an alternative to pyrolysis, produces hydrochar, which outperforms conventional pyrolysis in some ways, including the use of lower temperatures, and comparatively higher conversion yields (Masoumi et al., 2021). This is the first work to describe the synthesis of magnetic hydrochar (MH) from black liquor precursors using a low-temperature hydrothermal method as well as its application as an adsorbent for the removal of methylene blue from water. Magnetic particles were also added to the materials, which could be quickly removed from solution by a magnetic separator after usage (Li et al., 2021).
The aim of the study was to i) fabricate magnetic hydrochar from black liquor ii) investigate the impact of initial Fe^{3+} content and iii) assess the ability of magnetic hydrochar to adsorb methylene blue.

Paper Received: 24 June 2022; Revised: 14 July 2022; Accepted: 07 October 2022
Please cite this article as: Nguyen B.N., Nguyen N.H., Phan P.T., Phama T.C., Nguyen T.D., Phame N.S., Nguyen A.Q., 2022, Hydrothermal Conversion of Black Liquor to Magnetic Hydrochar and Its Potential for Methylene Blue Removal, Chemical Engineering Transactions, 96, 469-474 DOI:10.3303/CET2296079

2. Experimental

2.1 Materials

RS was obtained in Dong Thap Province (Mekong River Delta, Vietnam). Potassium hydroxide (KOH, ≥ 85 %), sodium hydroxide (NaOH, ≥ 97 %), iron (III) chloride hexahydrate ($FeCl_3.6H_2O$, ≥ 99 %), were purchased from Merck. MB ($C_{16}H_{18}N_3SCl.xH_2O$, 99.5 %), was obtained from Sigma - Aldrich. All chemicals used were of analytical grade and were used as received without any further purification.

2.2 Synthesis of magnetic hydrochar

In a typical procedure, RS was washed several times with distilled water and dried at 378 K before milling and being poured through 250 mesh sieves. Following that, 15 g of RS powder was immersed in 150 ml KOH 5 % solution. The mixture was transferred into a 250 mL Teflon-lined autoclave and placed in an oven at 393 K for 4 h. After cooling to room temperature, vacuum filtration is used to remove solids from the black liquor, which contains lignin and KOH. After slowly pouring 50 ml of $FeCl_3$ solution with various concentrations (0.5; 1.0 and 1.5 M) into 125 ml of the above solution for 2 h, hydrothermal treatment was performed at 453 K in 14 h. The obtained solid was washed with distilled water several times until the pH value reached neutral. Finally, the hydrochar was dried in an oven at 313 K in 12 h. The following rules were used to name the resulting samples: MH-x (x=1, 2 and 3, which refers to different concentrations of $FeCl_3$ solution at 0.5; 1.0 and 1.5 M, respectively). In addition, for comparison, hydrochar without $FeCl_3$ addition and a sample without black liquor were prepared, referred to as HC and FO, respectively.

2.3 Structure characterization

X-ray diffraction (XRD) was carried out ON X D8 Advance - Bruker with Cu K_α radiation (λ = 0,15418 nm). The Fourier transforminfrared (FTIR) spectroscopy was measured on IR Affinity-1S spectrophotometer (Shimadzu). The specific surface area (BET) was determined by N_2 adsorption–desorption isotherms at liquid nitrogen temperature (77 K) using a Quantachrome TriStar 3000 V6.07A adsorption instruments. The morphology was observed with S4800 - Hitachi scanning electron microscope (SEM). Energy-dispersive X-ray spectrum (EDS) was recorded on H7593 - Horiba. Magnetization measurements were carried out using a vibrating sample magnetometer (VSM) 7307 **-** Lake Shore. The UV-Vis spectrometry was recorded on Spectro UV-2650 (Labomed- USA) at wavelength of 664 nm.

2.4 Adsorption test

During our experiment, we measured adsorption capacity using conditions such as adsorbent/dye dose (1 g / 1 L MB), initial MB concentration (100 mg L^{-1}), contact time (90 min) and constant room temperature. When the adsorption reached equilibrium, it was separated with a magnet, and the residual MB in the solution was measured using UV - VIS. The following equation was used to calculate the adsorption capacity at time t, qt / mg g-1:

$$q_t = \left(\frac{C_0 - C_t}{m}\right) V \quad (1)$$

Where C_0 and C_t / mg L^{-1} are the initial and at time *t* concentrations of dye in the solution, respectively, *V* / L is the initial volume of the solution, and *m* / g is the dry mass of the adsorbent.

2.5 Reusability

In the reusability experiment, after the adsorption reached equilibrium, the adsorbent was magnetically separated and washed with a 0.1 M solution of HCl. The adsorption capacity was determined. The procedure was repeated 5 times to assess the potentially regenerable property of MH (Zeng et al., 2021). The relative capacity, *R* / % was expressed by the following equation:

$$R = \frac{q_{e,n}}{q_e} \times 100 \quad (2)$$

Where q_e and $q_{e,n}$ / mg g^{-1} is equilibrium adsorption capacity of the first and n^{th} cycle.

3. Results and Discussion

3.1 Structure characterization

In Figure 1a, the diffraction peaks of FO at 2θ = 24.51; 33.31; 35.90; 49.57; 53.95; 62.25; 63.81 ° correspond to crystalline hematite Fe_2O_3 (JCPDS 00-001-1053) and a broad peak at 2θ = 22 ° represents the crystalline of lignin and SiO_2 in biowaste (Zeng et al., 2021). These results demonstrate that ferric oxide or hydrochar cannot convert into magnetic materials after hydrothermal process.

The XRD of magnetic hydrochars, on the other hand, is completely different. The diffraction 2θ peaks at 30.46; 35.86; 43.58; 57.25; 62.65 ° are consistent with standard Fe_3O_4 (JCPDS 00-019-0629) and increase in intensity with increasing initial iron content, indicating that added Fe^{3+} ion is reduced into Fe_3O_4 in the hydrothermal process (Zeng et al., 2021).

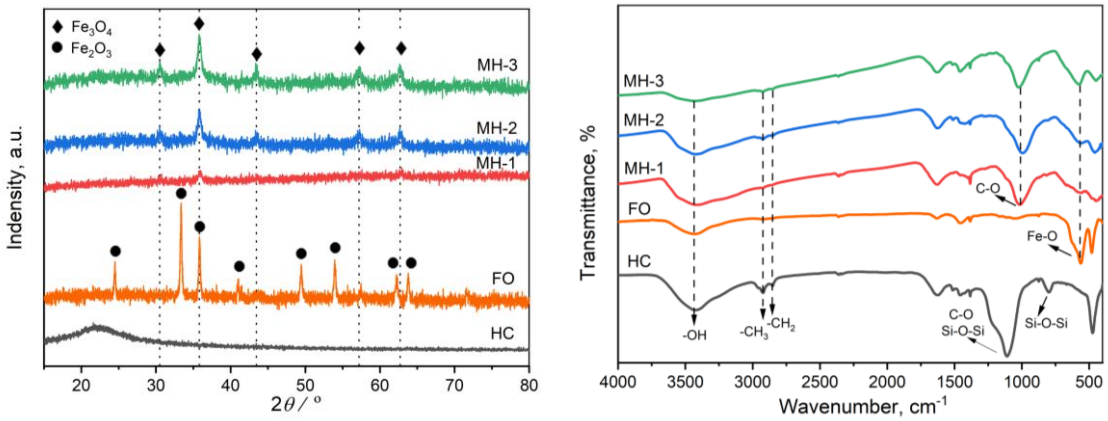

Figure 1: (a) XRD patterns and (b) FTIR spectra of HC, FO and MH samples

FTIR spectra of all samples revealed functional groups (Figure 1b). All five samples have a broad and strong band around at 3420 cm^{-1}, corresponding to -OH stretching vibrations (Li et al., 2020). Regarding HC and MH samples, the bands at 2920 cm^{-1} and 2850 cm^{-1} can be ascribed to the C-H stretching of methyl and methylene groups (Liu et al., 2021). In the case of HC, the characteristic absorption peaks at 1110 cm^{-1} and 798 cm^{-1} can be attributed to C-O stretching vibration of lignin; Si-O-Si stretching vibration and Si-O-Si bending vibration, respectively (Cheng et al., 2021). For the MH samples, the stretching vibration of C-O is shifted to 1000 cm^{-1} (Tong et al., 2021). Moreover, the stretching vibration of Fe-O bond was attributed to the gradual increase in peak intensity at near 560 cm^{-1} from MH-1 to MH-3 (Krishna Murthy et al., 2020).
At room temperature, the magnetic properties of three MH samples were measured using the VSM test. As shown in Figure 2a, the saturation magnetization value of MH-1; MH-2 and MH-3 are 18.97; 33.7 and 48.8 emu g^{-1}, respectively. This superparamagnetic property allows for the quick separation of adsorbents from aqueous solution. These findings correspond to XRD and FTIR results.

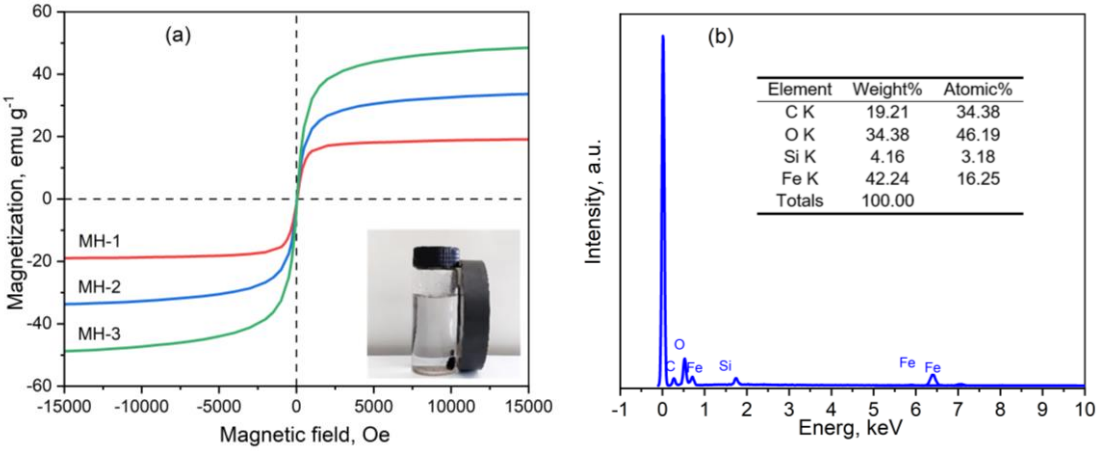

Figure 2: (a) Magnetization curves and illustration of the MH samples and (b) EDS spectrum and elemental analysis of MH-2 sample

The porous properties of RS and MH-2 were investigated by the nitrogen adsorption-desorption isotherms at 77 K are shown in Table 1. Rice straw had specific surface area (S_{BET}) and total pore volume (V_T) of 1.3 m^2 g^{-1} and 0.01 cm^3 g^{-1}, respectively. These values are minor, which is consistent with general properties of dry biomass (Siddiqui and Chaudhry, 2019). Interestingly, in MH-2 sample, there is a significant increase in S_{BET} = 171.4 m^2 g^{-1}; V_T = 0.146 cm_3 g^{-1}. According to the IUPAC classification, the nitrogen adsorption-desorption isotherm of MH-2 sample (Figure 3a) exhibits the Type IV isotherm and there is a magnetic hysteresis loop

between their adsorption and desorption branches, which indicated the presence of mesopores. Further, pore size of MH-2 (Figure 3b) is 5.96 nm (between 2 - 50 nm), demonstrating the presence of a mesopore structure in MH-2 (Ravikovitch and Neimark, 2001).

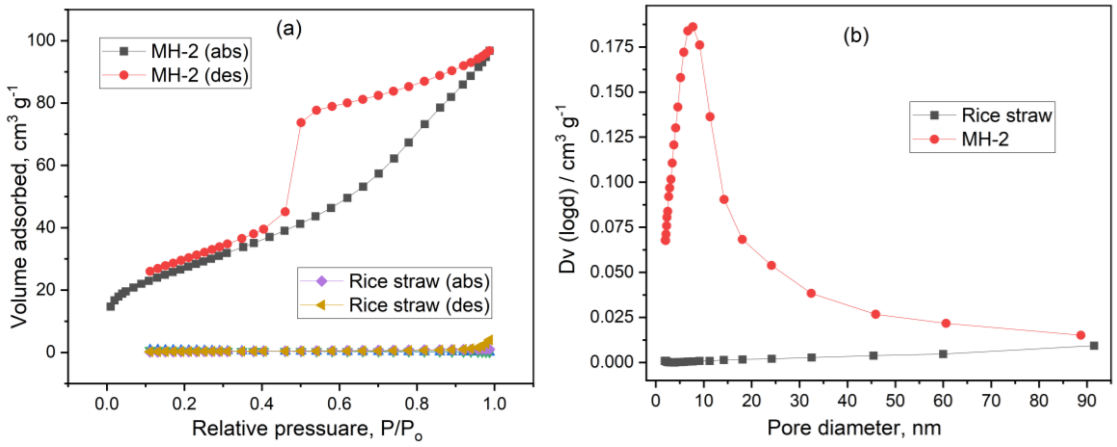

Figure 3: (a) Nitrogen adsorption-desorption isotherms (b) Pore size distribution of RS and MH-2 sample

Table 1: The porous parameters of rice straw and MH-2 sample

Sample	S_{BET} / m^2 g^{-1}	V_T / cm^3 g^{-1}	D_P / nm
Rice straw	1.3	0.006	30.66
MH-2	171.4	0.146	5.96

The morphology of rice straw and magnetic hydrochar was examined using SEM (Figure 4). The surface of rice straw was rough, while a typical SEM images of as-prepared MH with microsphere morphology and particle diameters ranging from 50 to 120 nm. EDS elemental analysis (Figure 2b) can confirm the existence of C (19.21 %), O (34.38 %), Fe (42.24 %) elements, indicating that Fe_3O_4 were formed in MH-2 sample.

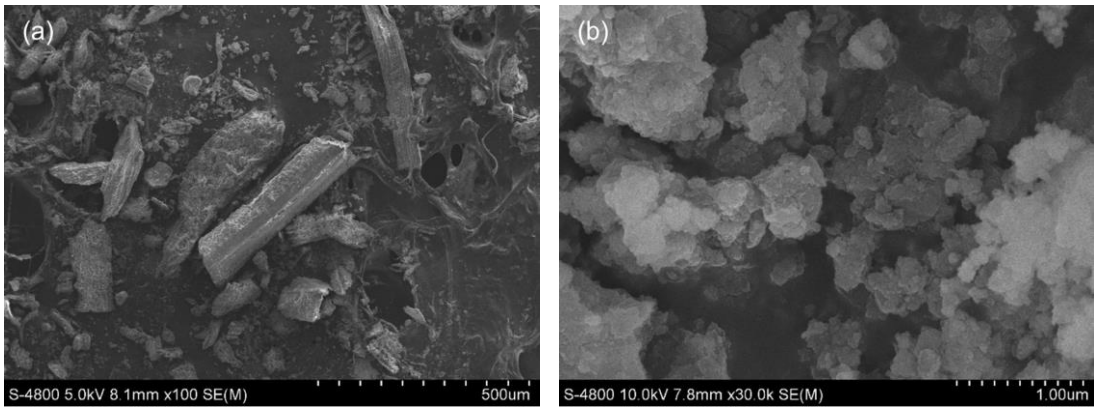

Figure 4: SEM images of (a) RS (b) MH-2

3.2 Adsorption efficiency for MB

During contact time studies, the adsorption of methylene blue was tested. Initially, the adsorption performance is rapid, achieving 84.13; 80.58; 65.97 % for MH-1, MH-2, MH-3, respectively of the total uptake in 10 min, which could be attributed to the abundance of uptake sites on the MH surface. While methylene blue molecules gradually occupied the binding sites, adsorption increased gradually and reached equilibrium in 30 min. Clearly, adsorption of MB on the surface of MH is physical (Anirudhan et al., 2012). Figure 5a also shows that the adsorption capacity of MH-1, MH-2, MH-3 is 98.07; 97.40 and 82.14 mg g-1 respectively, and inversely proportional to the amount of Fe3O4 as well as saturation magnetization in magnetic hydrochars. Thus, the MH-2 sample appears to be optimal in terms of adsorption capacity and magnetization. When compared to other materials regarding adsorption efficiency, saturation magnetization value

andsynthesis process, this experiment show significant potential in the field of magnetic adsorbents (Table 2). Moreover, when reusability of MH-1 and MH-2 is compared, MH-2 has an outstanding performance after 5 times of use, exhibiting MH-2 is one of the best choices among investigated samples.

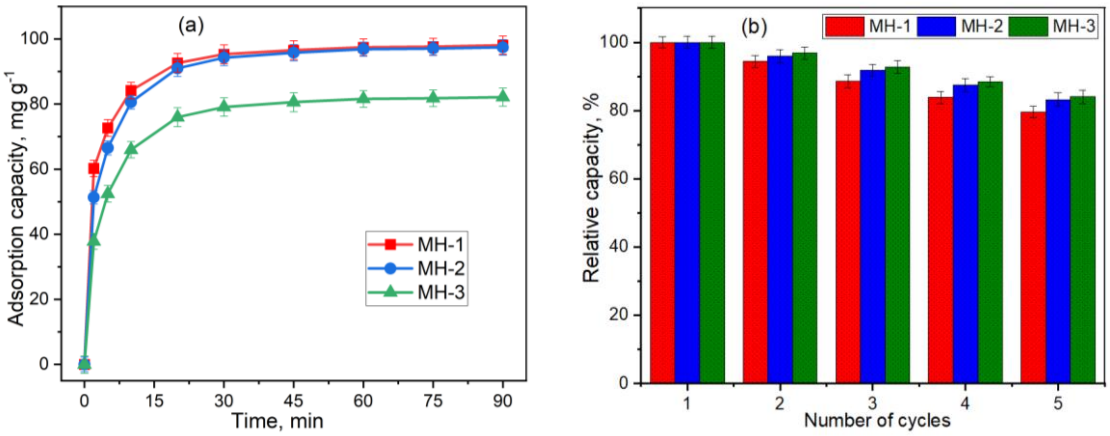

Figure 5: (a) Capacity during contact time and (b) Regeneration for MB adsorption onto MH samples

Table 2: The comparison of the magnetization and adsorption capacity of products with various hydrochars

Raw materials	Method	Magnetization, emu g^{-1}	Adsorption capacity, mg g^{-1}	References
Rice straw, $FeCl_3$, KOH	Hydrothermal 453 K, 14 h	18.97 - 48.80	98.07 - 82.14	This work
Coffee husk, $FeCl_3$, $FeSO_4$, NH_3	Hydrothermal 493 K, 6 h	7.05	78	(Krishna Murthy et al., 2020)
Pulp, $FeCl_3$	Hydrothermal 473 K, 1 h	2	11.03	(Saygili, 2019)
Fe $(NO_3)_3$, Ni $(NO_3)_2$, ethylene glycol, NaOH	Pyrolysis 1073 K, 2h	30.74	72	(Gayathri et al., 2019)
Chitosan, $FeCl_2$, $FeCl_3$, NH_3	Hydrolysis	22.7	50.37	(Türkeş and Sağ Açıkel, 2019)
$FeCl_2$, $FeCl_3$, NH_3, TEOS	Hydrolysis	58.7	43.15	(Jiaqi et al., 2019)

3.3 Reusability

Regeneration and recycling of magnetic hydrochars are critical for practical applications. As shown in Figure 5b, the MB uptake capacity of all three magnetic hydrochars gradually decreased as regeneration times increased. The adsorption capacity of the samples was maintained at approximately 79.56 % by MH-1; 83.19 % by MH-2 and 84.01 % by MH-3 after five cycles. This finding suggests that magnetic hydrochars have excellent performance and can be used to remove MB.

4. Conclusion

In this study, we reported a novel magnetic hydrochar derived from rice straw as an efficient and low-cost adsorbent for removing MB in aqueous solution. The magnetic properties of three magnetic hydrochars increase in proportion to the initial concentration of Fe^{3+}, whereas the adsorption capacity showed the opposite trend. With 1 M Fe^{3+} concentration, MH-2 is the best sample in terms of adsorption efficiency and saturation magnetization. Its removal efficiency for MB dye was rapidly high, indicating that it could be used as a potential materials in the field of magnetic adsorbents.

References

Anirudhan T.S., Nima J., Sandeep S., Ratheesh V.R.N., 2012, Development of an amino functionalized glycidylmethacrylate-grafted-titanium dioxide densified cellulose for the adsorptive removal of arsenic(V) from aqueous solutions, Chemical Engineering Journal, 209, 362-371.

Cheng L., Ji Y., Liu X., 2021, Insights into interfacial interaction mechanism of dyes sorption on a novel hydrochar: Experimental and DFT study, Chemical Engineering Science, 233.

Gayathri M.B., Mathangi J.B., Raji P., Helen K.M., 2019, Equilibrium and kinetic studies on methylene blue adsorption by simple polyol assisted wet hydroxyl route of NiFe2O4nanoparticles, Journal of Environmental Health Science & Engineering, https://doi.org/10.1007/s40201-019-00368-9.

Jiaqi Z., Yimin D., Danyang L., Shengyun W., Liling Z., Yi Z., 2019, Synthesis of carboxyl-functionalized magnetic nanoparticle for the removal of methylene blue, Colloids and Surfaces A: Physicochemical and Engineering Aspects, 572, 58-66.

Krishna Murthy T.P., Gowrishankar B.S., Krishna R.H., Chandraprabha M.N., Mathew B.B., 2020, Magnetic modification of coffee husk hydrochar for adsorptive removal of methylene blue: Isotherms, kinetics and thermodynamic studies, Environmental Chemistry and Ecotoxicology, 2, 205-212.

Le V.X., Lee H., Pham N.S., Bong S., Oh H., Cho S.-H., Shin I.-S., 2021, Stainless steel 304 needle electrode for precise glucose biosensor with high signal-to-noise ratio, Sensors and Actuators B: Chemical, 346.

Li J., Zhang Y., Wang F., Wang L., Liu J., Hashimoto Y., Hosomi M., 2021, Arsenic immobilization and removal in contaminated soil using zero-valent iron or magnetic biochar amendment followed by dry magnetic separation, Sci Total Environ, 768, 144521.

Li Y., Zimmerman A.R., He F., Chen J., Han L., Chen H., Hu X., Gao B., 2020, Solvent-free synthesis of magnetic biochar and activated carbon through ball-mill extrusion with Fe3O4 nanoparticles for enhancing adsorption of methylene blue, Sci Total Environ, 722, 137972.

Liu T., Chen Z., Li Z., Fu H., Chen G., Feng T., Chen Z., 2021, Preparation of magnetic hydrochar derived from iron-rich Phytolacca acinosa Roxb. for Cd removal, Sci Total Environ, 769, 145159.

Masoumi S., Borugadda V.B., Nanda S., Dalai A.K., 2021, Hydrochar: A Review on Its Production Technologies and Applications, Catalysts, 11(8).

Pham N.S., Le V.X., 2022, 4-dimethylaminopyridine: Discovery of a co-reactant system providing outstanding and reliable emission in electrochemiluminescence, Journal of Electroanalytical Chemistry, 921, 116507.

Pham N.S., Phan P.T.Q., Nguyen B.N., Le V.X., 2022, Enhanced stability of electrochromic devices based on Prussian blue by tuning electrolyte ions and charge/discharge balance, Journal of Applied Electrochemistry, 89.

Ravikovitch P.I., Neimark A.V., 2001, Characterization of nanoporous materials from adsorption and desorption isotherms, Colloids and Surfaces, 187–188, 11–21.

Saygili H., 2019, Hydrothermal synthesis of magnetic nanocomposite from biowaste matrix by a green and one-step route: Characterization and pollutant removal ability, Bioresour Technol, 278, 242-247.

Sharma H.B., Sarmah A.K., Dubey B., 2020, Hydrothermal carbonization of renewable waste biomass for solid biofuel production: A discussion on process mechanism, the influence of process parameters, environmental performance and fuel properties of hydrochar, Renewable and Sustainable Energy Reviews, 123.

Siddiqui S.I., Chaudhry S.A., 2019, Nanohybrid composite Fe2O3-ZrO2/BC for inhibiting the growth of bacteria and adsorptive removal of arsenic and dyes from water, Journal of Cleaner Production, 223, 849-868.

Tawfik A., Nasr M., Galal A., El-Qelish M., Yu Z., Hassan M.A., Salah H.A., Hasanin M.S., Meng F., Bokhari A., Qyyum M.A., Lee M., 2021, Fermentation-based nanoparticle systems for sustainable conversion of black-liquor into biohydrogen, Journal of Cleaner Production, 309.

Titchou F.E., Zazou H., Afanga H., El Gaayda J., Akbour R.A., Hamdani M., 2021, Removal of Persistent Organic Pollutants (POPs) from water and wastewater by adsorption and electrocoagulation process, Groundwater for Sustainable Development, 13.

Tong S., Shen J., Jiang X., Li J., Sun X., Xu Z., Chen D., 2021, Recycle of Fenton sludge through one-step synthesis of aminated magnetic hydrochar for Pb(2+) removal from wastewater, J Hazard Mater, 406, 124581.

Türkeş E., Sağ Açıkel Y., 2019, Synthesis and characterization of magnetic halloysite–chitosan nanocomposites: use in the removal of methylene blue in wastewaters, International Journal of Environmental Science and Technology, 17(3), 1281-1294.

Valderrama O.J., Zedda K.L., Velizarov S., 2021, Membrane Filtration Opportunities for the Treatment of Black Liquor in the Paper and Pulp Industry, Water, 13(16).

Yağmur H.K., Kaya İ., 2021, Synthesis and characterization of magnetic ZnCl2-activated carbon produced from coconut shell for the adsorption of methylene blue, Journal of Molecular Structure, 1232.

Zeng H., Qi W., Zhai L., Wang F., Zhang J., Li D., 2021, Magnetic biochar synthesized with waterworks sludge and sewage sludge and its potential for methylene blue removal, Journal of Environmental Chemical Engineering, 9(5).

Zhang Z., Wang T., Zhang H., Liu Y., Xing B., 2021, Adsorption of Pb(II) and Cd(II) by magnetic activated carbon and its mechanism, Sci Total Environ, 757, 143910.